Acta Crystallographica Section B
Structural Science
ISSN 0108-7681

Synthesis, structure, and stability of the high-temperature 6H-type perovskite phase $Ba_3BaSb_2O_9$

Chris D. Ling,[a,b]* Maxim Avdeev[b] and Karina Aivazian[a]

[a]School of Chemistry, The University of Sydney, Sydney 2006, Australia, and [b]Bragg Institute, ANSTO, PMB 1, Menai 2234, Australia

Correspondence e-mail: c.ling@chem.usyd.edu.au

Received 27 March 2007
Accepted 19 April 2007

The structure of $Ba_3BaSb_2O_9$ is reported for the first time as a high-temperature phase with an ideal hexagonal $BaTiO_3$-type structure (space group $P6_3/mmc$) and Rietveld-refined against high-temperature synchrotron X-ray powder diffraction data. The structure is remarkable for the extreme size difference between the pairs of face-sharing $Sb^{5+}O_6$ octahedra (with mean Sb—O bonds of 1.99 Å) and the single corner-sharing $Ba^{2+}O_6$ octahedra (with mean Ba—O bonds of 2.46 Å), which is greater than for any other reported 6H perovskite. This is consistent with the very different ionic radii of Sb^{5+} (0.60 Å) and Ba^{2+} (1.35 Å), and accounts for the instability of this phase at room temperature. The known symmetry-lowering modes of closely related 6H perovskites such as $Ba_3SrNb_2O_9$ and $Ba_3SrTa_2O_9$ are considered, but found not to account for the behaviour of $Ba_3BaSb_2O_9$ on cooling from high temperatures.

1. Introduction

Perovskites containing large cations such as Ba^{2+} in the 12-fold coordinate *A* sites have long been of interest for their extreme structural and compositional flexibility, suggesting possible applications such as nuclear waste-form matrices. Many of the Ba^{2+} *A*-site perovskites adopt the hexagonal 6H perovskite-type structure of $BaTiO_3$, in which BaO_3 layers are stacked in an *hcchcc* sequence that results in pairs of face-sharing TiO_6 octahedra alternating with single corner-sharing TiO_6 octahedra. Blasse (1965) reported lattice parameters for a number of 2:1 *B*-site cation-ordered 6H perovskites, $Ba_3A^{2+}Sb_2^{5+}O_9$, *A* = Mg, Ca, Sr, Ba, Co, Ni, Cu and Zn. Of these phases, the structures of $Ba_3MgSb_2O_9$ (Lufaso *et al.*, 2005; Treiber & Kemmler-Sack, 1982), $Ba_3CoSb_2O_9$ (Doi *et al.*, 2004; Istomin *et al.*, 2004), $Ba_3NiSb_2O_9$ (Doi *et al.*, 2004; Kohl & Reinen, 1977), $Ba_3CuSb_2O_9$ (Kohl & Reinen, 1977) and $Ba_3ZnSb_2O_9$ (Lufaso *et al.*, 2005) have since been reported in the ideal hexagonal $BaTiO_3$-type space group $P6_3/mmc$; the monoclinically distorted structure of a further phase $Ba_3MnSb_2O_9$ has been reported in $C2/c$. However, to the best of our knowledge there have been no further reports in the literature of *A* = Ca, Sr or Ba.

Here, we report the structure of $Ba_4Sb_2O_9$ (*i.e.* *A* = Ba) for the first time as a high-temperature phase with an ideal hexagonal $BaTiO_3$-type structure. This phase is remarkable for the extreme size difference between the pairs of face-sharing $Sb^{5+}O_6$ octahedra and the single corner-sharing $Ba^{2+}O_6$ octahedra, which is larger than for any other reported 6H perovskite. The stability of this phase at room temperature is discussed in terms of the known symmetry-lowering modes of other 2:1 *B*-site cation ordered 6H perovskites.

2. Synthesis and characterization

In the course of an exploratory solid-state synthetic investigation of the Ba–Sb–O system, an unexpected phase was obtained. It was found to have a 2:1 ratio of Ba:Sb by energy-dispersive X-ray analysis (EDXA), performed in conjunction with imaging using a Phillips XL-30 scanning electron microscope (SEM) with a tungsten filament operating at 20 keV, a spot size setting of 5 and a working distance of 11 mm. A pure sample was subsequently synthesized by conventional solid-state reaction; a stoichiometric mixture of Sb_2O_3 (Aldrich, 4N) and $BaCO_3$ (Aldrich, 3N8) were ground together in an agate mortar and heated to 1073 K for 12 h, reground and heated again to 1073 K for 12 h (all heating and cooling at 15 K min^{-1}).

Conventional (Cu $K\alpha$) X-ray diffraction (XRD) data were collected on a Shimadzu XRD-6000 diffractometer, for a sample that appeared to be homogeneous by EDXA. Although the pattern was difficult to index due to poor peak shapes and considerable overlap among weak peaks, the strongest peaks could be indexed to a primitive hexagonal unit cell with $a \simeq 6.12$, $c \simeq 15.99$ Å. This composition and unit cell corresponded approximately to $Ba_4Sb_2O_9$, reported by Blasse (1965) as a hexagonal $BaTiO_3$-type (6H) perovskite, implying that Sb^{3+} had oxidized to Sb^{5+}. Further synthetic and XRD investigations revealed that the crystallinity of the samples could be considerably improved by quenching to room temperature from 1073 K, suggesting that between the annealing temperature (1073 K) and room temperature, $Ba_4Sb_2O_9$ undergoes one or more phase transitions to lower symmetries that are poorly crystalline and hence extremely difficult to determine. This may explain why, to the best of our knowledge, there have been no reports of $Ba_4Sb_2O_9$ in the literature since the original report by Blasse. In order to properly characterize this phase for the first time, we therefore collected variable-temperature high-resolution synchrotron XRD data as described in §3.

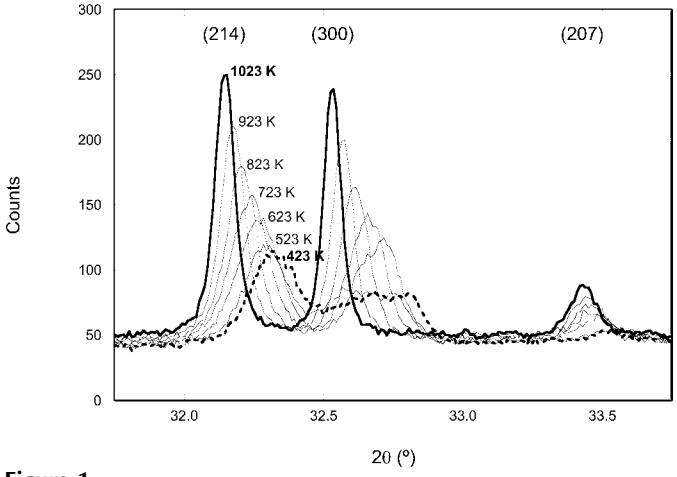

Figure 1
Variable-temperature synchrotron XRD data (λ = 1.000617 Å) for $Ba_4Sb_2O_9$ showing the improvement in crystallinity with increasing temperature, with some evidence of a phase transition below ∼ 573 K. Labelled peak indices correspond to the high-temperature $P6_3/mmc$ phase.

Table 1
Experimental details.

Crystal data	
Chemical formula	$Ba_4Sb_2O_9$
M_r	936.81
Cell setting, space group	Hexagonal, $P6_3/mmc$
Temperature (K)	1023
a, c (Å)	6.18123 (8), 15.9900 (3)
V (Å^3)	529.09 (2)
Z	2
D_x (Mg m^{-3})	5.8787 (2)
μ (mm^{-1})	11.369
Specimen shape	Cylinder
Specimen size (mm)	20 × 0.3
Specimen colour	White
Data collection	
Radiation type	Synchrotron
Wavelength (Å)	1.000617 (7)
2θ range (°)	5–85
2θ increment (°)	0.01005
Measurement device	Image plate
Measurement method	Debye–Scherrer
Absorption correction	Cylinder (Lobanov & Alte da Veiga, 1998)
Refinement	
R_p	0.0284
wR_p	0.0367
χ^2	0.0960
No. of reflections used	7808
No. of parameters refined	64
Computer program	*GSAS* (Larson & Von Dreele, 1994)
Profile function	Pseudo-Voigt

3. Synchrotron XRD data collection

Synchrotron XRD data were collected at the Australian National Beamline Facility (ANBF), Photon Factory, Tsukuba, Japan. The polycrystalline sample was finely ground and loaded into glass capillaries with an internal diameter of 0.3 mm, which were rapidly spun during data collection. Two imaging plates were used to collect the powder diffraction data in Debye–Scherrer geometry from 5–45 and 45–85 °2θ, respectively. All measurements were performed under vacuum to minimize air scatter. The divergence of the beam in the direction of 2θ was 0.002 Å and the sample-to-imaging plate distance was 573 mm. The wavelength was determined to be 1.000612 (7) Å by Rietveld refinement of a pattern collected from a Si standard (NBS640C) under the same conditions.

The sample was heated using a resistive tube furnace around the entire length of the capillary, with a narrow window at the beam position to allow data collection. A Weissenberg screen was used in combination with a translating imaging-plate cassette so that a number of exposures could be taken at different temperatures using the same set of imaging plates. Each exposure yielded a strip 100 pixels wide which, when extracted and integrated, gave a powder diffraction profile with step increments of 0.01005° 2θ.

Data were collected in 100 K steps from 423–1023 K (close to the highest temperature available using this furnace). Peak

Table 2
Selected bond lengths (Å) and bond-valence sums (BVS; Brese & O'Keeffe, 1991) for the refined structure of $Ba_4Sb_2O_9$ at 1023 K.

	Bond length (Å)	BVS		Bond length (Å)	BVS
Sb1		5.354	Ba1		1.045
Sb1—O1 (×3)	1.943 (12)		Ba1—O1 (×6)	3.0957 (8)	
Sb1—O2 (×3)	2.028 (10)		Ba1—O2 (×3)	3.115 (10)	
			Ba1—O2 (×3)	3.750 (10)	
Ba3		1.413			
Ba3—O1 (×6)	3.043 (13)		Ba2		3.769
Ba3—O2 (×6)	3.1134 (18)		Ba2—O1 (×6)	2.458 (12)	
O1		1.993	O2		2.008

shapes narrowed significantly with increasing temperature (Fig. 1) and there was evidence of a phase transition or decomposition at $\sim$573 K. Patterns collected above this temperature could be fully indexed in the ideal 6H perovskite space group $P6_3/mmc$, but those collected below this temperature had severely degraded peak shapes with possible signs of splitting at reflections such as (300) in Fig. 1. Unfortunately, despite the high resolution of the synchrotron XRD data, the low-temperature data were still of insufficient quality to unambiguously determine the space group and unit cell. Specific attempts were made to fit the additional peaks by reducing the symmetry to $P6_3/m$, as reported for $Ba_3Sr(Nb,Ta)_2O_9$ at room-temperature (Zandbergen & Ijdo, 1983), and $C2/c$, as reported for $Ba_3MnSb_2O_9$ at room temperature (Doi *et al.*, 2004), but neither space group could model the experimentally observed additional reflections. The structure refinements described in §4 therefore concentrate exclusively on the high-temperature high-symmetry phase of $Ba_4Sb_2O_9$.

4. Structure determination and refinement

The highest-temperature (1023 K) data set was chosen for structure determination and Rietveld refinement because it appeared to be the most crystalline based on full widths at half-maximum (FWHM). The starting model was an ideal 6H perovskite with face-sharing $Sb^{5+}O_6$ octahedra and edge-sharing $Ba^{2+}O_6$ octahedra of identical size and Ba^{2+} cations in the *A* sites.

The Rietveld refinement was carried out using the *GSAS* program (Larson & Von Dreele, 1994) with the EXPGUI front-end (Toby, 2001). The 5–45 and 45–85° 2θ data sets were used in the refinement. Scale factors, zero-shifts, background functions (shifted Chebyschev as implemented in *GSAS* with 20 terms) and peak-shape parameters (pseudo-Voigt function 'type 2' as implemented in *GSAS*, refining only the Gaussian parameter GW and the two Lorentzian parameters LY and LZ) were refined independently for each data set.

The unit-cell parameters and a global isotropic atomic displacement parameter (ADP) were initially refined along with the instrumental parameters described above. Atomic positions were then refined, leading to a significant expansion of the $Ba^{2+}O_6$ octahedra relative to the $Sb^{5+}O_6$ octahedra.

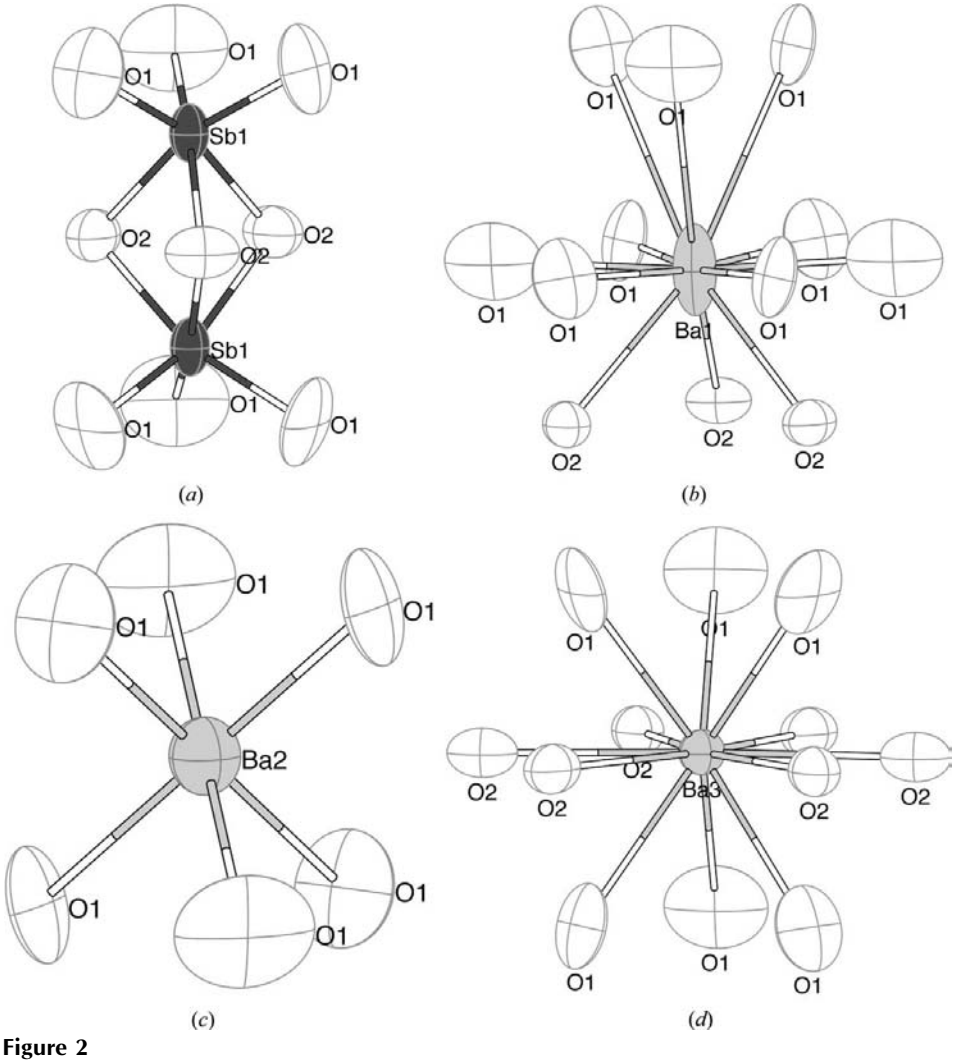

Figure 2
Displacement ellipsoid plots (50% probability) showing the coordination environments of (*a*) Sb1, (*b*) Ba1, (*c*) Ba2 and (*d*) Ba3 at 1023 K.

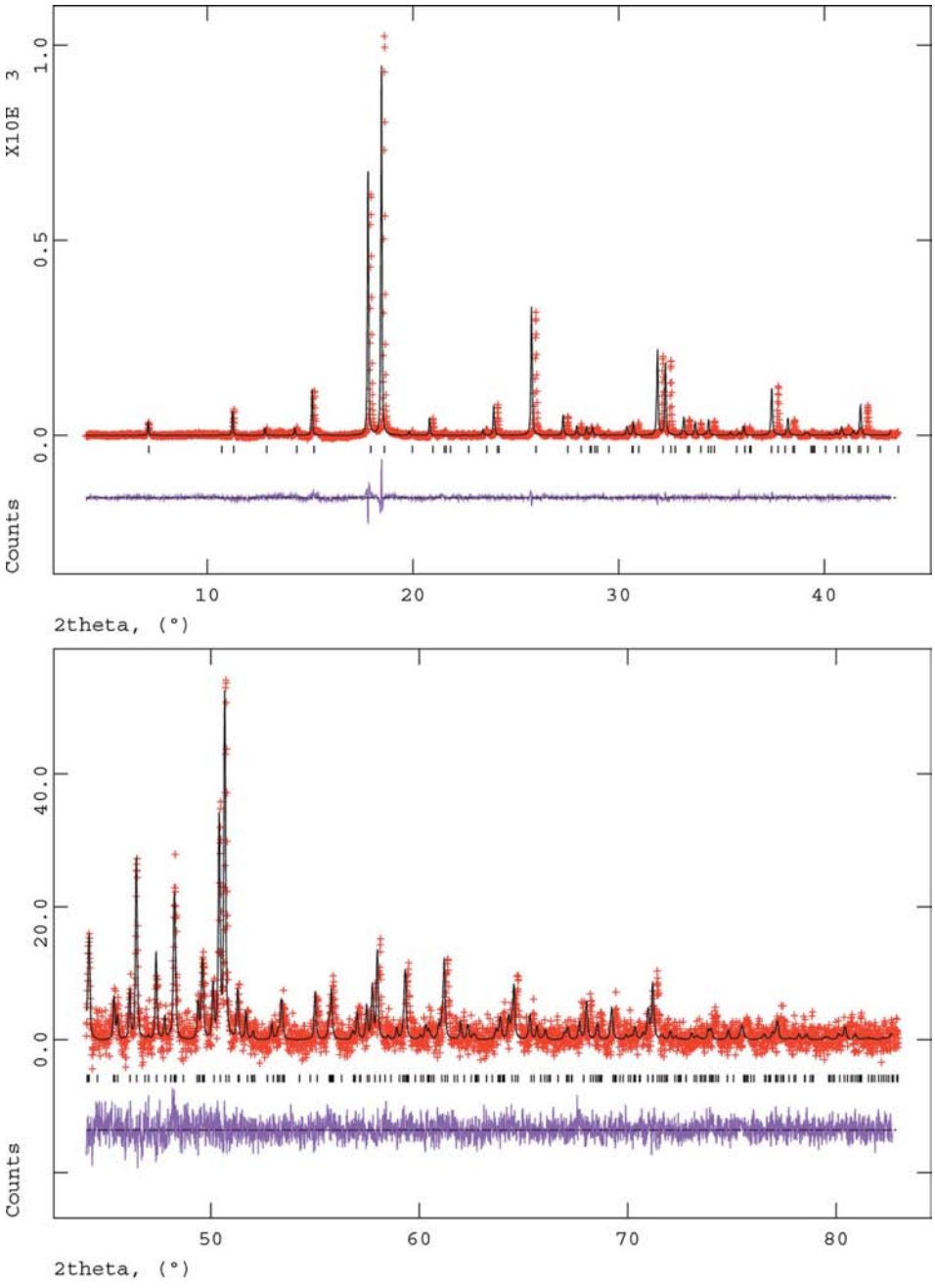

Figure 3
Observed (crosses), calculated (solid line) and difference (below) synchrotron XRD profiles of $Ba_4Sb_2O_9$ at λ = 1.000617 Å and T = 1023 K.

Refinement of independent ADPs for each site led to negative ADPs for Sb1, which were corrected by applying the empirical absorption correction for cylindrical samples of Lobanov & Alte da Veiga (1998), as implemented in *GSAS*.

In the final cycles, anisotropic ADPs were also refined, giving stable and chemically reasonable results. ADPs for all atoms remained quite isotropic with two exceptions: O1, which is bonded to Ba2 to form BaO_6 octahedra (Fig. 2*c*), shows evidence for displacements perpendicular to the Ba—O bond, and Ba1, which sits in a very elongated 12-fold coordinate *A* site (note the long bonds to O1 in Fig. 2*b*) show evidence for displacements along the axis of elongation (*c*). A trial Rietveld refinement was made with Ba1 modelled as a split site along this axis, but this did not lead to improved residuals.

Finally, an attempt was made to lower the symmetry of the refined model to $P6_3/m$, as reported for $Ba_3Sr(Nb,Ta)_2O_9$ at room temperature (Zandbergen & Ijdo, 1983), allowing the octahedra to rotate about the *c* axis. This resulted in small distortions but only a very slight reduction in the residuals: R_p dropped from 0.0284 to 0.0273, R_{wp} dropped from 0.0367 to 0.0365, and χ^2 dropped from 0.0960 to 0.0952. Even given the relatively small contribution of the O atoms to the X-ray pattern compared with the heavy metals Sb and Ba, this reduction in residuals could not be considered a statistically significant improvement for the introduction of five new parameters to the refinement, and the $P6_3/mmc$ space group has been used to report the final refined structure.

Full experimental details and final refinement statistics are presented in Table 1, with the final Rietveld fit shown in Fig. 3. The final refined structure parameters have been deposited.[1] The structure is shown in polyhedral representation in Fig. 4. The local coordination of metal atoms is shown in Fig. 2 as 50% probability displacement ellipsoid plots, with bond lengths and empirical bond-valence sums (BVS; Brese & O'Keeffe, 1991) in Table 2.

5. Discussion

The most striking feature of the refined structure of $Ba_4Sb_2O_9$ shown in Fig. 3 is the very large size difference between SbO_6 and BaO_6 octahedra, with average M—O bond distances of 1.981 (16) and 2.456 (12) Å, respectively (Table 2). This was expected on the basis of their very different ionic radii (IR). In sixfold coordination environments at room temperature,

[1] Supplementary data for this paper are available from the IUCr electronic archives (Reference: AV5086). Services for accessing these data are described at the back of the journal.

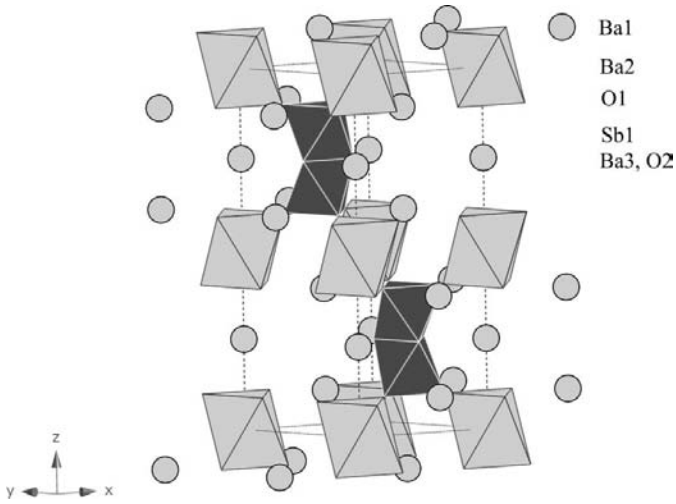

Figure 4
Polyhedral representation of the refined structure of $Ba_4Sb_2O_9$ at 1023 K. SbO_6 octahedra are dark grey, BaO_6 octahedra are light grey and Ba spheres are light grey.

IR(Sb^{5+}) = 0.60 Å while IR(Ba^{2+}) = 1.35 Å (Shannon, 1976), which is a larger ionic size difference than occurs in any other reported 6H perovskite, almost certainly accounting for its instability at room temperature. The closest analogues would be $Ba_4Nb_2O_9$ and $Ba_4Ta_2O_9$, where IR(Nb^{5+}) = IR(Ta^{5+}) = 0.64 Å. Phases of these compositions were originally reported as cubic perovskites (Blasse, 1965), but later (Kemmler-Sack *et al.*, 1981) as high-temperature phases with an oxygen-deficient 5H perovskite structure (in the case of $Ba_4Nb_2O_9$) and an orthorhombically distorted hexagonal perovskite structure (in the case of $Ba_4Ta_2O_9$). Neither structure was fully determined nor (to the best of our knowledge) has either phase been reported since, suggesting that like $Ba_4Sb_2O_9$, they are either metastable at room temperature or undergo symmetry-lowering phase transitions accompanied by severe degradation in crystallinity.

Calculated empirical bond-valence sums (BVS; Brese & O'Keeffe, 1991) provide further insight into the instability of $Ba_4Sb_2O_9$ at room temperature. Although the parameters used to calculate BVS have been empirically determined on the basis of published oxide structures at room temperature, and their validity is therefore not guaranteed at high temperature, the results for the refined structure of $Ba_4Sb_2O_9$ at 1023 K (Table 2) are sufficiently striking to merit some discussion. Calculated BVS for Sb^{5+} and O^{2-} ions are reasonably close to their expected values. However, the calculated BVS for $Ba2^{2+}$ of 3.769 is nearly double its expected value, indicating that it is extremely overbonded in its octahedral coordination environment (Fig. 1*c*). At the same time, the calculated BVS of $Ba1^{2+}$, which sits on a perovskite *A* site that has been elongated along *z* by the enlarged $Ba2O_6$ octahedra (Fig. 2*b*), is severely underbonded with a calculated BVS of 1.045. $Ba3^{2+}$, which sits in the more regular perovskite *A* site (Fig. 2*d*) is less severely underbonded with a calculated BVS of 1.413.

Zandbergen & Ijdo (1983), in their study of the 6H perovskites $Ba_3SrNb_2O_9$ and $Ba_3SrTa_2O_9$ at room temperature, found evidence for a symmetry-lowering from $P6_3/mmc$ to $P6_3/m$. They argued that this symmetry lowering, which permits octahedral rotations about the *c* axis, arises to relieve the underbonding of the perovskite *A* sites when the ratio of lattice parameters *c*/*a* is significantly larger than the ideal ratio of $6^{1/2} \simeq 2.45$. They noted that the values of *c*/*a* at room temperature for $Ba_3SrNb_2O_9$ (2.533) and $Ba_3SrTa_2O_9$ (2.523) were larger than for any other well characterized hexagonal perovskite, owing to the large size of Sr^{2+} (IR = 1.18 Å) compared with Nb^{5+} and Ta^{5+} (IR = 0.64 Å; see Table 3 of Zandbergen & Ijdo, 1983). In the case of $Ba_4Sb_2O_9$ at 1023 K, as has already been noted, the corresponding size difference is considerably greater, as is the ratio of *c*/*a* = 2.587. Furthermore, *c*/*a* = 2.613 for the (poorly crystalline) sample of $Ba_4Sb_2O_9$ at room temperature. Nevertheless, no evidence was found for a symmetry lowering to $P6_3/m$ at 1023 K nor did the weak additional peaks at room temperature correspond to this space group. It appears that octahedral rotations of this type are insufficient to relieve the extreme underbonding of Ba1 (and to a lesser extent Ba3) in this case, leading to either a different symmetry lowering to a space group yet to be determined and/or to decomposition of the phase.

Synchrotron XRD data were collected at the Australian National Beamline Facility (ANBF) at the Photon Factory, Japan, with the assistance of Dr James Hester and the financial support of the Australian Synchrotron Research Program (ASRP).

References

Blasse, G. (1965). *J. Inorg. Nucl. Chem.* **27**, 993–1003.
Brese, N. E. & O'Keeffe, M. (1991). *Acta Cryst.* B**47**, 192–197.
Doi, Y. S., Hinatsu, Y. & Ohoyama, K. (2004). *J. Phys. Condens. Matter*, **16**, 8923–8935.
Istomin, S. Y., Koutcenko, V. A., Antipov, E. V., Lindberg, F. & Svensson, G. (2004). *Mater. Res. Bull.* **39**, 1013–1022.
Kemmler-Sack, S., Thumm, I. & Herrmann, M. (1981). *Z. Anorg. Allg. Chem.* **479**, 177–183.
Kohl, P. & Reinen, D. (1977). *Z. Anorg. Allg. Chem.* **433**, 81–93.
Larson, A. C. & Von Dreele, R. B. (1994). *GSAS.* Los Alamos National Laboratory, New Mexico, USA.
Lobanov, N. N. & Alte da Veiga, L. (1998). 6th European Powder Diffraction Conference, 22–25 August. Abstract P12-16. Budapest, Hungary.
Lufaso, M. W., Hopkins, E., Bell, S. M. & Llobet, A. (2005). *Chem. Mater.* **17**, 4250–4255.
Shannon, R. D. (1976). *Acta Cryst.* A**32**, 751–767.
Toby, B. H. (2001). *J. Appl. Cryst.* **34**, 210–213.
Treiber, U. & Kemmler-Sack, S. (1982). *Z. Anorg. Allg. Chem.* **487**, 161–177.
Zandbergen, H. W. & Ijdo, D. J. W. (1983). *Acta Cryst.* C**39**, 829–832.